

Chapter 2

Role of Renewable Energy and its Classifications

2.1. Introduction

In the last chapter, the aspects of Sustainable Development (SD) focused on Renewable Energy (RE) resources exploitation have been elaborated. It has been reported that RE sources would improve the human life and minimize the consequences of global warming. Figure 1.1, states that to achieve emission level to 14 Gt, one of the major focus is to be non-biomass based renewables. It has been reported that solar energy and bio-energy based engineering systems are on top most priority. This chapter has been focused on three major aspects of RE sources and has been briefed as under:

- a) Role of Solar Energy resources with Photovoltaic (PV) technologies.
- b) Utilization of Concentrated Solar Power (CSP) for industrial applications.
- c) Microalgae based Bio-energy is targeted for Carbon emissions capture.

2.2. Role of Solar Energy

Out of various commercially available Solar technologies, PV technology has been studied using its mathematical model and the effect of dynamic weather conditions has been considered as inputs. The State Space Analysis control of PV model has been described for stability and a SIMULINK model has been developed for an industrial site and simulated for dynamic weather conditions.

2.2.1. Mathematical Modeling of PV cell/ Module/Array

A mathematical model for a PV system has been developed and its performance analysis has been reported. The equivalent electrical circuit of a real Solar cell with series resistance and shunt resistance has been shown in the Figure 2.1. A solar cell is an electronic device which directly converts sunlight into electricity or also called as "light-generated current". Further to generate electrical power, a voltage is also generated by solar cell through a process called "Photovoltaic Effect". Semiconductor materials on the commercial applications primarily have been used for photovoltaic energy conversion [36].

The I-V curve of a solar cell is the superposition of the I-V curves of the solar cell diode in two scenarios first in the dark and second in the light-

generated current. The light has the effect of shifting the I-V curve down into the fourth quadrant where power can be extracted from the diode [37].

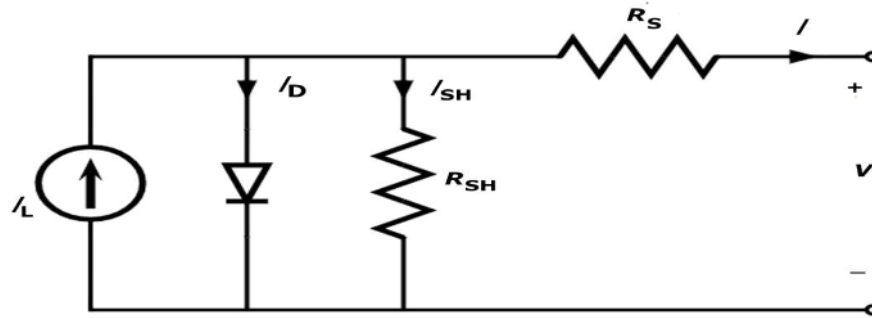


Figure. 2.1. Equivalent circuit of a real Solar PV cell

Illuminating a cell adds to the normal 'dark' currents in the diode so follows the famous Shockley diode Equation (2.1) [36]:

$$I = I_L - I_o \left[\exp\left(\frac{qV}{\eta kT}\right) \right] \quad (2.1)$$

where, I_L =light generated current, I_o =dark saturation current, η =Ideality Factor, T = Temperature in °K, V =Cell voltage. The ideality factor of a diode is a measure of how closely the diode follows the ideal diode equation.

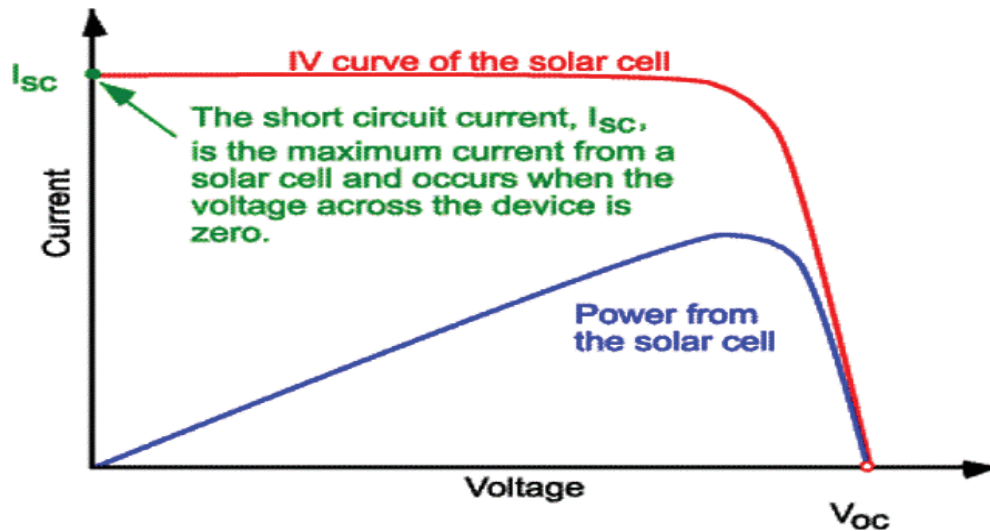


Figure. 2.2. Current-Voltage Curves showing I_{sc} and V_{oc} of a Solar cell

Further, the Equation (2.1) is based on assumption that at lower voltage the I_L dominates the I_o , which is specific case of very low illumination and also based on constant ideality factor. However in real situation the ideality factor is reported as function of diode voltage. It has been also evaluated that the ideality factor approaches 'one' at higher voltage and of 'two' at low diode voltage [38].

The I_{SC} is due to the generation and collection of light-generated carriers shown in Figure 2.2. For an ideal Solar cell at most moderate resistive loss mechanism, the I_{SC} and the light-generated current I_L are identical. Therefore, the I_{SC} is the largest current which may be drawn from the Solar cell.

2.2.2. Five Parameters based Single Diode Model

In real silicon Solar Cell, the recombination components are the function of carrier orientation and diode model parameters. This is basically a limitation of the double diode model and so the 'five' parameters based single diode model has been selected for mathematical modeling [37].

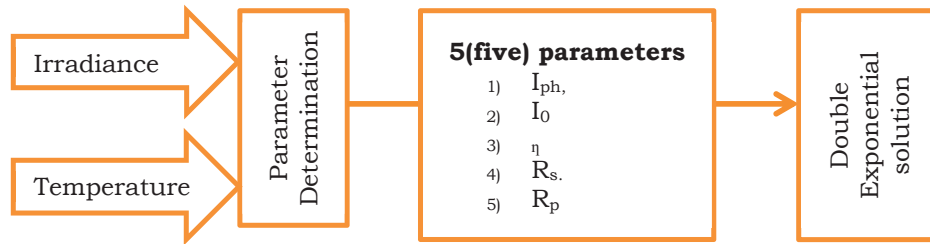


Figure. 2.3. Schematic diagram of '5' parameter block representation

Based on reported studies, the performance of any PV model is predicted by three solar-cell variables of the I_{SC} , the V_{OC} , and the values of Voltage (V_{MP}) and Current (I_{MP}) that correspond to the maximum power (P_{MAX}) point on the curve. However, the mathematical equation for any PV cell is represented by double exponential with five major parameters has been shown by Equation (2.2).

$$I = I_{ph} - I_{01} \left\{ \exp \left[\frac{q(V + IR_S)}{kT} \right] - 1 \right\} - I_{02} \left\{ \exp \left[\frac{q(V + IR_S)}{kT} \right] - 1 \right\} - \frac{(V) + IR_S}{R_{SH}} \quad (2.2)$$

where I_{ph} is the photo-generated current, I_{01} and I_{02} are saturation current due to recombination in the quasi-neutral regions and the depletion region respectively. q is the basic electron charge, whereas k is the Boltzmann constant = 1.38×10^{-23} J/K, and T is the absolute cell temperature. R_S and R_{SH} represents the resistances between metallic contacts and leakage of the current across the p-n junction [37].

It has been also reported that number of diodes in equivalent model increases the levels of complexity and classified as single diode single exponential and double diode double exponential respectively. For drawing the I-V curve, Newton-Raphson method has been reported as preferred by most of

researchers due to its simplicity [39]. Research studies have reported that the PV system output has linearly dependence on the solar cell area, solar irradiance intensity and cell temperature. Equation (2.3) shows the interrelation between phase current, temperature and solar irradiance [39]:

$$I_{Ph} = I_{Ph,STC} * \frac{G}{G_{STC}} * [1 + \alpha_I(T - T_{STC})] \quad (2.3)$$

Where α_I is the current temperature coefficient at STC and accordingly, the I-V characteristics take the form shown in Figure 2.4, whereas V_t is the thermal diode voltage as shown in Equation (2.5)

$$I = I_{Ph} - I_{Sat} * \left(e^{\frac{V}{kV_t} - 1} \right) \quad (2.4)$$

$$V_t = \frac{kT}{q} \quad (2.5)$$

k the Boltzmann constant, q the electron charge, & η is the cell ideality factor. The saturation current is expressed as follows:

$$I_{Sat} = C * T^3 * e^{\left(\frac{E_{gap}}{kT} \right)} \quad (2.6)$$

where E_{gap} is the band gap of the semiconductor material and C is the temperature coefficient.

The R_S and R_{SH} effects the Solar cell productivity which is commonly referred by cell fill factor. The fill factor (FF) is defined as the ratio between two quantity of product of V_{MPP} and I_{MPP} values and product of I_{SC} and V_{OC} values.

$$FF = \frac{V_{MPP} * I_{MPP}}{V_{OC} * I_{SC}} \quad (2.7)$$

The I-V characteristic curve of Solar cell has been analyzed based on its device, material/electrical properties. The I-V characteristics of a PV cell working in uniform conditions have been plotted in Figure 2.4.

The general characteristic for a PV device using the two-diode model is as given in Equation (2.2) and the illumination generated current from the PV cell directly depends linearly on solar irradiation and the temperature. The diode saturation current I_S also having the dependence on the temperature and on the saturation current density of the semiconductor and the active area of the cells.

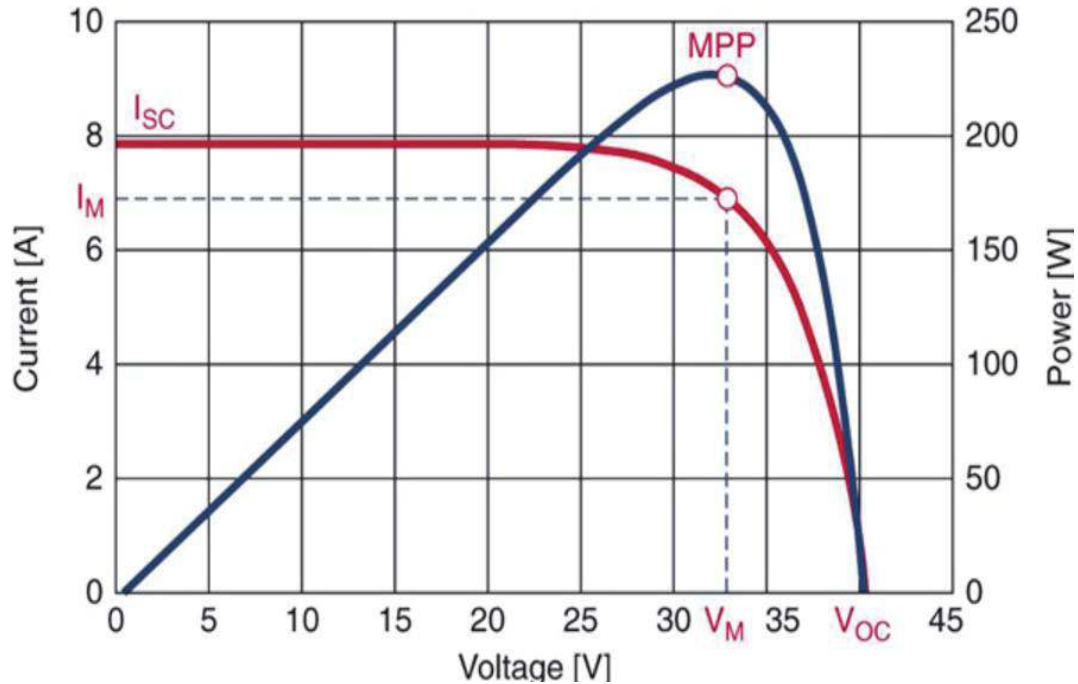


Figure. 2.4. Current and Power vs Voltage characteristic curve of solar cell[40]

$$I_S = I_{S,ref} \left[\frac{T_n}{T} \right]^3 \exp \left\{ \frac{qE_g}{ak} \left(\frac{1}{T_n} - \frac{1}{T} \right) \right\} \quad (2.8)$$

The current depends on the intrinsic material characteristics of the cell and various parameters like the coefficient of electron-diffusion for the semiconductor, life-period of minority carriers, and the intrinsic carrier density. The Equation (2.8) suggests that these parameters do effect the efficiency of the solar cell.

2.2.3. Temperature and Radiation Effects

Temperature and Solar irradiance are reported as two important factors which affects the I-V characteristics considerably. The variation further varies the Maximum Power Point (MPP) on the I-V curve as shown in Figure 2.5 due to dynamic weather conditions. These changes of MPP results in great power loss and power generated from PV system has been not transferred to the load.

In any PV system, maximum power point tracking (MPPT) is an important aspect which enables maximum energy extraction from an array using logic algorithms controlled by feedback sensors. From the Figure 2.6, current and voltage changes as irradiance and temperature vary [41]. The MPPT algorithms continuously search the MPP on the I-V curve and helps in the transfer of maximum power to load.

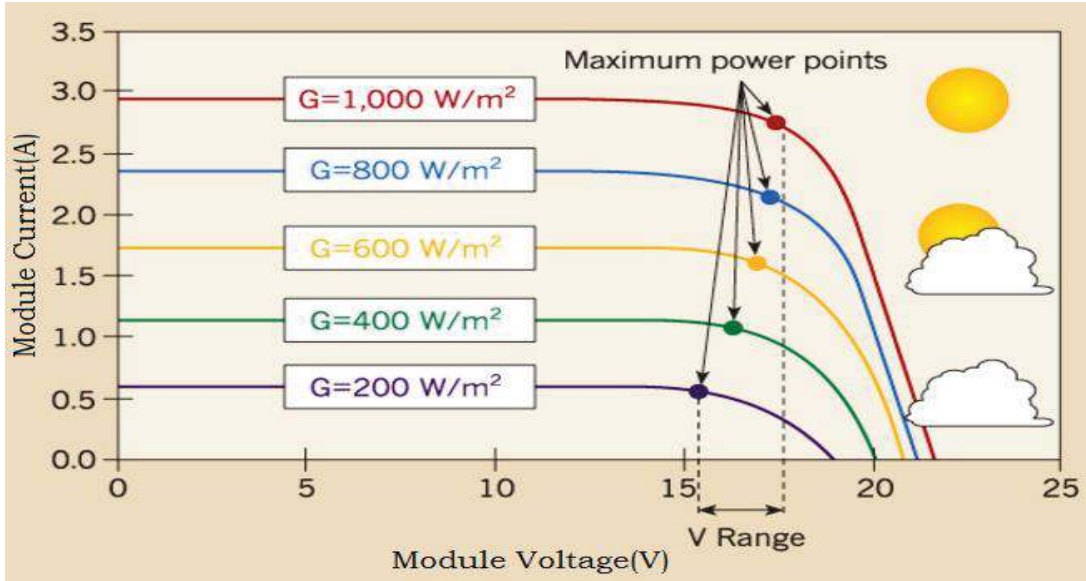


Figure. 2.5. PV module's I-V Characteristics with the varying irradiance [42]

The net effect on V and I is positive with the rise in irradiance and the P_{MAX} is generated. It is known that, at the fixed density of the current generated in a cell, the $V_{OC} = f(T)$ dependence is, practically, a linear function in the near to room temperature range and referred as below Figure 2.5.1 [43]. The required p-n junction overheating temperature in conditions of the thermal balance at any regime of connecting the cell to the external load is the temperature difference. The cell temperature disturbs the module generated voltage and the V_{OC} is directly and linearly dependent on the temperature as shown in Figure 2.5.1.

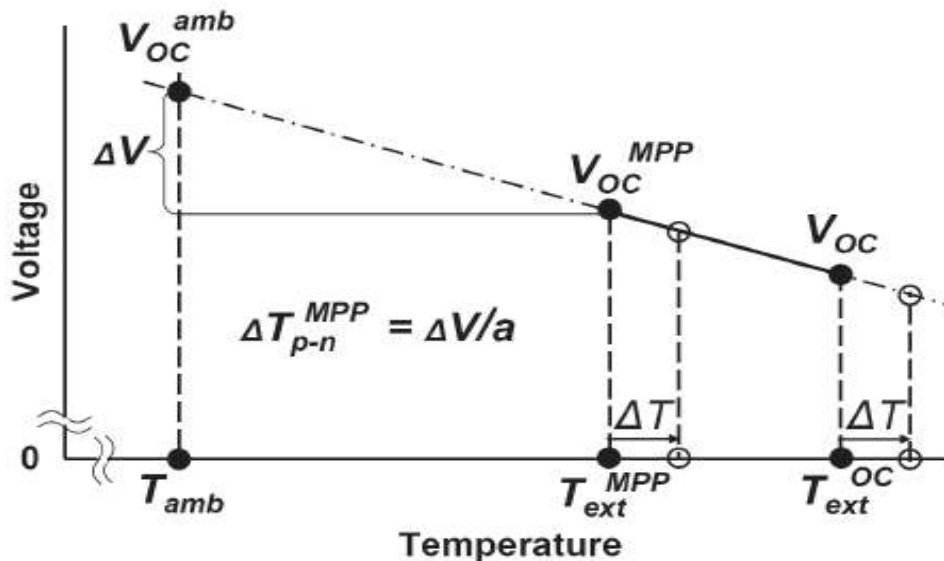


Figure 2.5.1 : Variation of Voltage with respect to temperature [43]

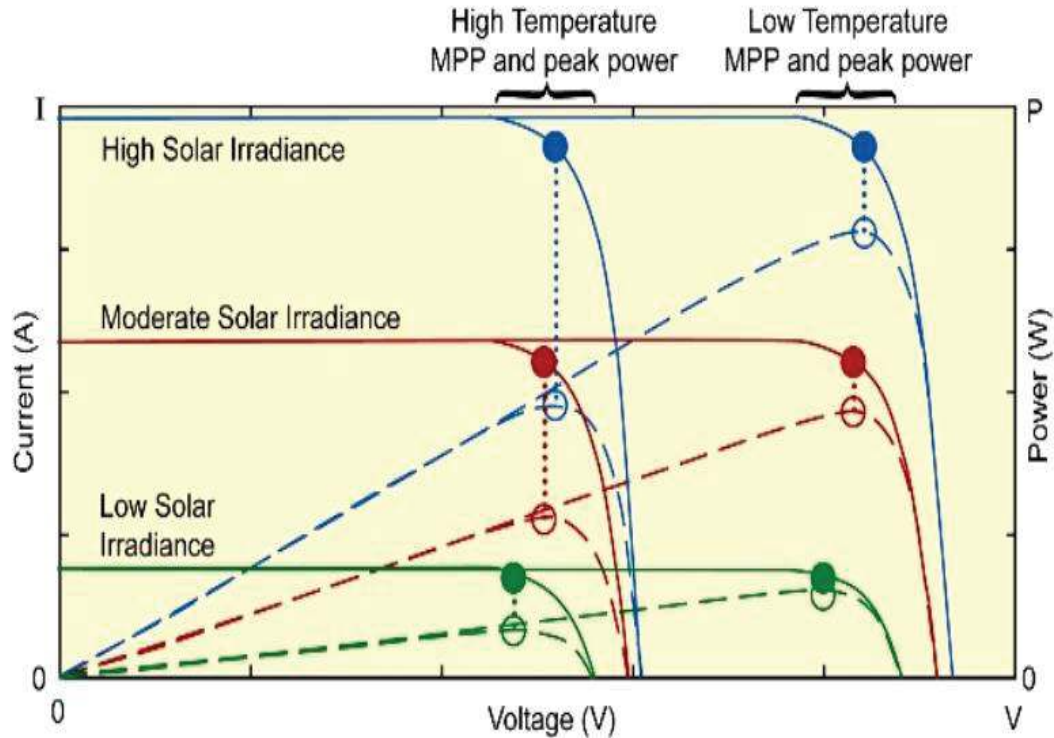


Figure. 2.6. I-V curves dynamics with irradiance and temperature [42]

It has been reported that I_{SC} is directly proportional to the irradiance and when operating point is not the short circuit, the I_{PH} is also the main factor in the module's current. Hence it has been essential to track the MPP in weather conditions to fix that the maximum power is obtained from the PV panel, which requires the use of DC-DC Converter. The duty ratio designs the control ability of converter and which controls and maintain the output voltage with the maximum power transfer to load. In modern converter, this task has been entrusted to the MPPT algorithms and being reported as major function of DC-DC converter, which behaves as an interface between load and PV module for transferring the maximum power generated from module [44].

2.2.4. DC-DC converters

PV panel characteristics are similar to a non-linear power source, which means that the output load DC power depend on the MPP on the I-V curve. Converters have capability of increasing or decreasing the magnitude of the output DC voltage and also invert its polarity. This is being achieved by the Pulse Width Modulation (PWM) technique, usually by constant frequency and the duty cycle, which is the ratio of the Conduction Time (T_{ON}) to Switching

period (T_s). The basic operating configurations of converters are Continuous Conduction Mode (CCM) and Discontinuous Conduction Mode (DCM) [45].

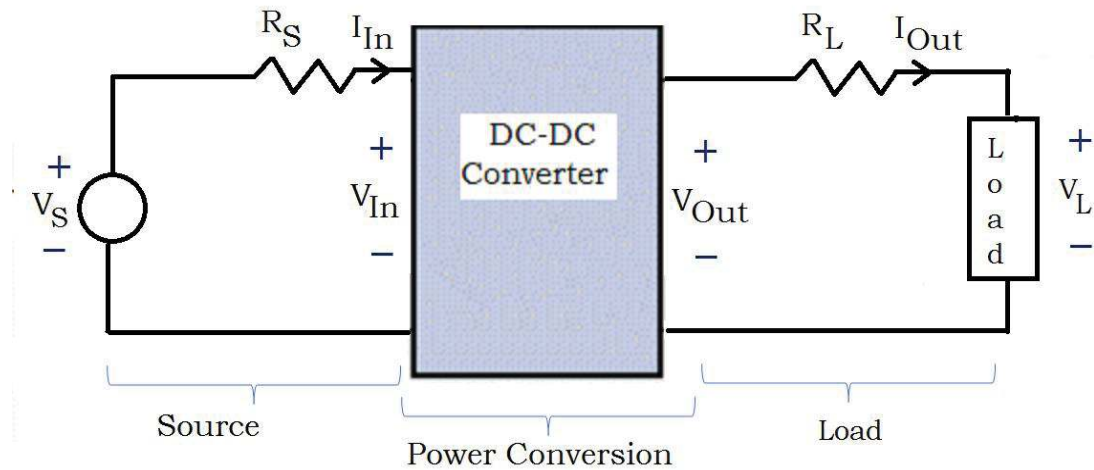


Figure. 2.7. Schematic on the concept of DC-DC converter

Power electronics device, the converter has the input resistance similarity which is actually proportional or inversely proportional to the switching frequency as shown in Figure 2.7. The most common DC to DC converters used with Solar PV system are Buck, Boost, Buck-Boost, Cuk and Sepic. However there are many other converters which are developed for solar PV system requirements. Different topologies of converters are further reported into isolated or non-isolated classifications. Fang Lin Luo and Hong Ye (2004) have reported six generations classification and more than 500 topologies of converters. A DC/DC converter family is shown in Appendix A [46]. The detailed deliberation on Power electronics is beyond the scope of present work.

2.2.5. Cuk Converter Topology

Converters have been also called as Charge Controllers, which maximizes the energy generated. Converter circuit elements are based on power electronics and have the non-linear components and produce harmonics in output waveforms and affect the system efficiency and duty cycle. Out of converters topologies, few converters utilize the storage elements like coupling capacitors to transfer the same energy with reduced harmonics and better output profile. Cuk converter is based on this dual principle which has been analyzed focused on current balance of the capacitor. Cuk converter has capability of providing the negative polarity regulated output voltage with respect to the input voltage. The

output voltage magnitude could be equal, more or lesser than the input, which depends on the duty cycle [47]. Utilizing these uniqueness, Cuk converter has been selected for the research analysis in this thesis.

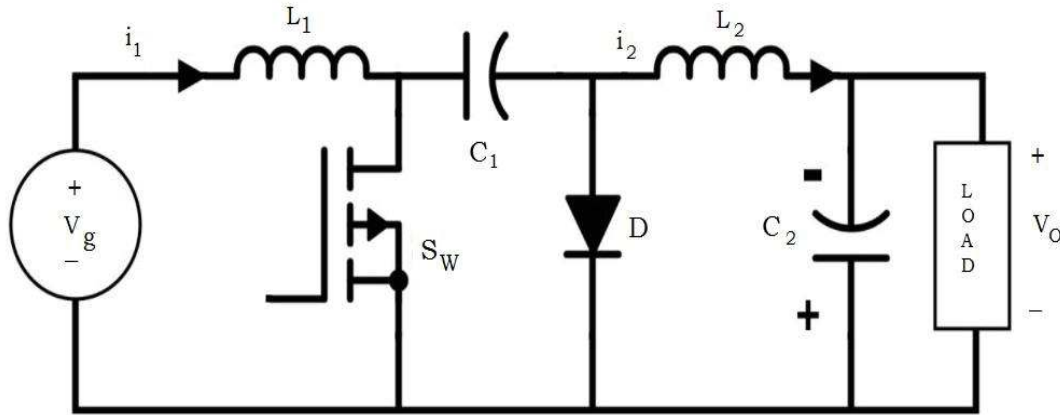


Figure. 2.8. Circuit diagram of a Cuk converter

The storage inductor (L_1) on the input side acts as the filter for the input DC supply (V_g) and to protect from large order harmonic content. Here, the primary capacitor (C_1) acts as energy storing element and continuously transferring the energy from the input to output. The basic electrical circuit of Cuk converter has been shown in Figure 2.8. The detailed analysis of converters and other power electronics devices are not in the scope of the thesis, however a brief has been provided in the present work. The circuit analysis of Cuk Converter has been based on assumptions:

- Both inductors have higher Inductance /Capacitor value and the flowing currents / voltages across are constant and switches are ideal
- The circuit is operating in the steady state i.e. V and I waveforms are periodic.
- For the duty ratio of D , closing time is DT and opening time is $(1-D)T$.

2.2.6. Role of Maximum Power Point Tracking Techniques

DC converters as charge controllers are further classified often called as PWM controller, which basically works as a switch between solar array and the load like battery. PWM controllers don't adjust for better efficiency during dynamic weather conditions [27]. Further the other type of charge controllers termed as MPPT techniques, which adjusts MPPs more accurately and increases

the output efficiency. The basic concepts of MPPT have been summarized for the readers.

The commonly utilized MPPT techniques have been briefed with basic double-diode model which emulates the PV characteristics equitably and accurately. It is derived that a direct-coupled PV system utilizes maximum to 31% of the PV capacity and approximately 97% of the PV power improvement has been achieved utilizing MPPTs [45]. MPPT is an electronic device inserted between the PV array and the load. Three major factors responsible for the performance of any MPPT are classified as the dynamic response, steady state error and tracking efficiency and also lead to the development of new or modification of existing control algorithms [48]. Two major conventional MPPT techniques, Perturb & Observe (P&O) and Incremental Conductance (INC) are briefed in this Chapter. For the present work the INC algorithm is utilized.

2.2.6.1 Perturb and Observe Algorithm

Due to simplified structure and easy implementation ways, the P&O algorithm has been reported as most common MPPT algorithm among the other techniques. The basic idea of control is to find out the MPP on the P-V curves of Solar cell, such that the difference of power ($\Delta P_{PV} = 0$) of the array. The periodical perturbation (plus or minus) of PV array terminal voltage or current is constantly compared with the value of previous disturbance. Then the output power of array is compared $P(n+1)$ with that at the last perturbation $P(n)$. To achieve MPP, signs of ΔP and ΔV are assessed every interval and depending upon their sign, the duty ratio is varied as reflected in Figures 2.9 and 2.10.

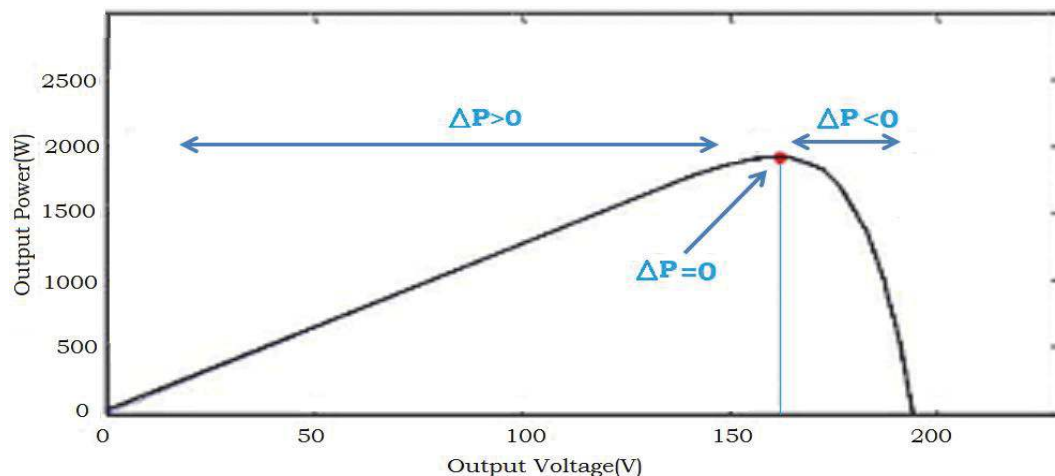


Figure. 2.9. Sign of the ΔP and ΔV on the I-V characteristic curve

While operating at MPP, solar panel is operated from V_{OC} and voltage is gradually decreased until maximum power point is achieved. The advantages of this technique are simplicity, ease of implementation and it does not require a previous knowledge of the PV array. However, the P&O will not stop perturbing when the MPP is reached and will oscillate around it resulting in some unnecessary power loss.

At low irradiation levels, the P&O algorithm exhibits a poor efficiency. In this work the dynamic weather conditions have been targeted, accordingly the other method of Incremental Conductance algorithm has been selected.

2.2.6.2 Incremental Conductance (INC) method

The incremental conductance technique was proposed in the year 1996 by researchers and this method is based on the fact that, the derivative of PV array output power with respect to its output voltage is zero ($dP / dV = 0$) at the MPP and at any irradiation and temperature level. It is negative on the right of MPP and positive on the left of the MPP as reflected in Figure 2.11. The flowchart shown in Figure. 2.12, suggest that the MPP is reached when the instantaneous conductance (I/V) is equal to the incremental conductance ($\Delta I / \Delta V$).

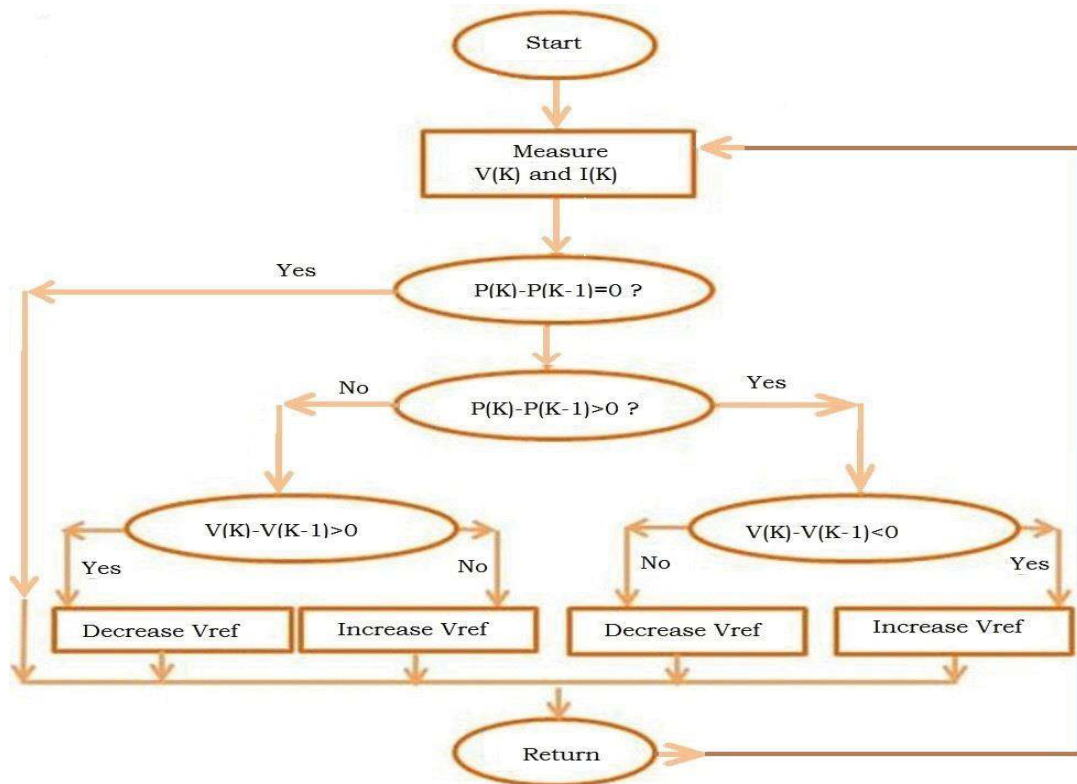


Figure. 2.10. Flowchart of the P&O algorithm

Once the MPP is reached, the PV array continues to operate at this point until change in ΔI is measured. This change in ΔI will correlate with the change in atmospheric condition and MPP.

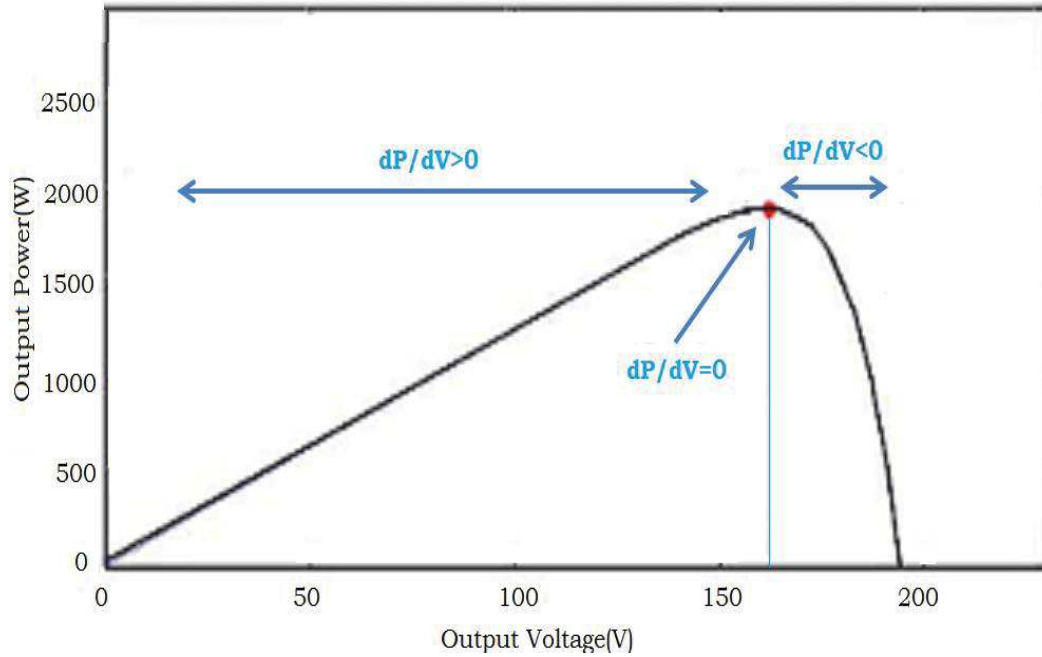


Figure. 2.11. Derivative of power with respect to voltage defines MPP (INC)

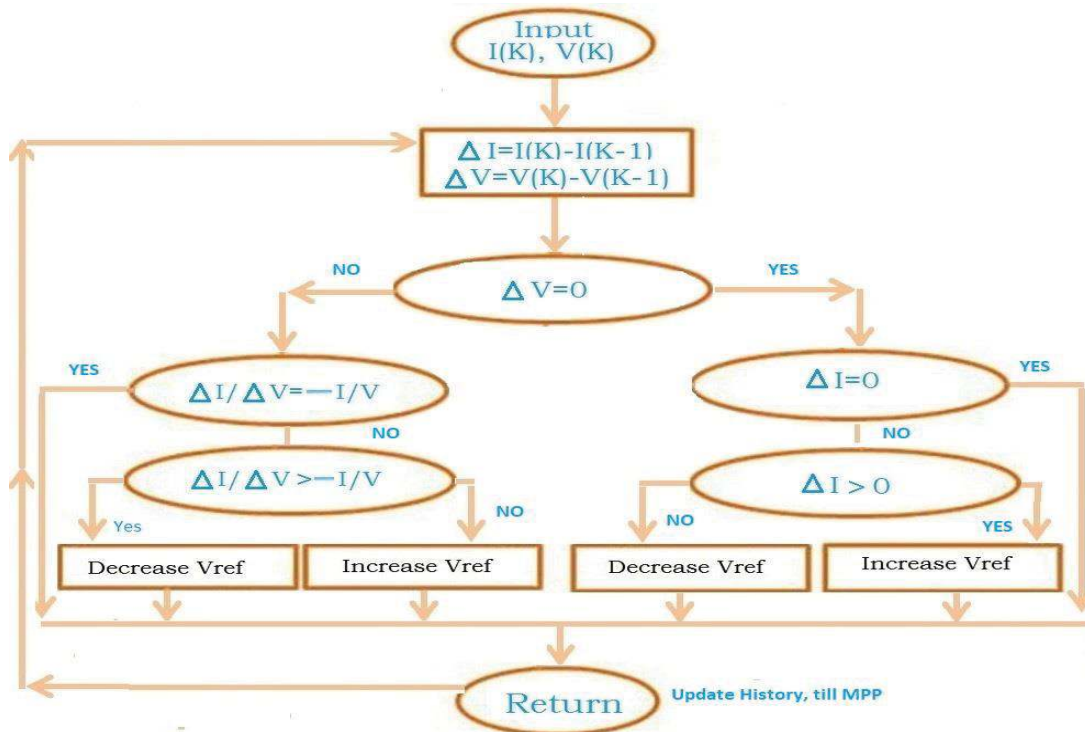


Figure. 2.12. Flowchart of the incremental conductance algorithm.

Hence, the algorithm increments or decrements the PV array operating voltage to track the MPP. When $(\Delta I / \Delta V < - I / V)$ the algorithm is operating on the right of MPP therefore, the array operating voltage is decreased to move the operating point towards the MPP. When $(\Delta I / \Delta V > - I / V)$ the algorithm is operating on the left of MPP hence the array operating voltage is increased.

However, the array operating voltage does not need any change once the MPP is reached at $(\Delta I / \Delta V = - I / V)$. INC technique has the advantages of no oscillation around the MPP during steady-state conditions, conversely, it performs erratically during transient conditions too [49].

Various comparison studies reported that on the basis of MPPT efficiency, the P&O and INC techniques have the potential to perform better than other techniques. The major MPPT techniques broadly classified as Online, Offline and Other methods as shown in Figure 2.13. These methods are differed based on important factors like working simplicity, number of sensors, cost effectiveness, efficiency range, convergence-speed and hardware implementation.

The conversion of output DC voltage to AC voltage has been the next step in PV system which has been performed by the use of an inverter. It requires appropriate electrical and electronics devices like switching, control circuits and transformers. Established technologies like solid state inverters do not have any moving elements and has been used in wide range solar PV systems.

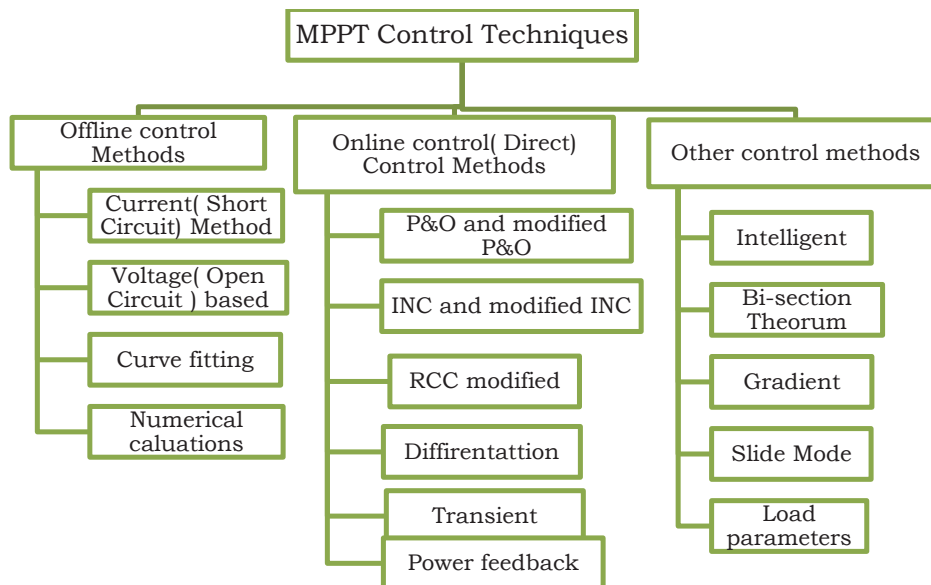


Figure. 2.13. Broad classifications of various MPPT techniques.

A power inverter, or inverter, is an electronic device or circuitry that changes direct current to alternating current. The input voltage, output voltage and frequency, and overall power handling depend on the design of the specific circuitry. Inverters based on low, medium and large applications are known as Micro inverters, String Inverters and Central Inverters respectively. The differences between these inverters are focused on their working methodologies, maintenance strategy, cost per watt, efficiency, robustness, voltage level, and safety hazards [50]. Inverters are further classified, when input DC voltage remains constant, then it is called Voltage Source Inverter (VSI), whereas when the input current required being constant, termed as Current Source Inverter (CSI). In this work standard PWM-VSI has been selected from SIMULINK directory.

The dynamic behavior of a PV system requires controlled output. State-space- averaging approach has been reported as a tool to analyze for the small-signal characteristics of PWM-controlled converters. The state equations and output equation reveal the characteristics of the particular physical system.

2.2.1. State Space analysis of Cuk Converter control

The fundamental equations for state space analysis [51] ‘x’ defines the state variables of the system and the ‘u’ variables defines the inputs. The number of states is defined by the number of storage elements in the system, as four states for the Cuk converter. The output voltage of the converter is the voltage across the capacitor C_2 as shown in Figure 2.9. The set of equations defines the Converter under ON / OFF stages of switch are briefed in Table 2.1.

Table 2.1. Cuk Converter equations under Switch ON and OFF situations

Situation	Set of governing equations	
Switch ON	$L_1 \frac{di_1}{dt} = V_g$	$L_2 \frac{di_2}{dt} = -V_1 - V_o$
	$C_1 \frac{dV_1}{dt} = i_2$	$C_2 \frac{dV_o}{dt} = i_2 - \frac{V_o}{R}$
Switch OFF	$L_1 \frac{di_1}{dt} = V_g - V_1$	$L_2 \frac{di_2}{dt} = -V_o$
	$C_1 \frac{dV_1}{dt} = i_1$	$C_2 \frac{dV_o}{dt} = i_2 - \frac{V_o}{R}$

With small perturbations are applied on the Switch ON conditions,

$$\begin{bmatrix} \hat{i}_1 \\ \hat{i}_2 \\ \hat{v}_1 \\ \hat{v}_0 \end{bmatrix} = \underbrace{\begin{bmatrix} 0 & 0 & 0 & 0 \\ 0 & 0 & -1/L_2 & -1/L_2 \\ 0 & 1/C_1 & 0 & 0 \\ 0 & 1/C_2 & 0 & -1/RC_2 \end{bmatrix}}_{A_1} \begin{bmatrix} i_1 \\ i_2 \\ V_1 \\ V_0 \end{bmatrix} + \underbrace{\begin{bmatrix} 1/L_1 \\ 0 \\ 0 \\ 0 \end{bmatrix}}_{B_1} [V_g]$$

$$\text{So, } \hat{x} = [A_1]x + [B_1]u$$

With small perturbations are applied on the Switch OFF conditions,

$$\begin{bmatrix} \hat{i}_1 \\ \hat{i}_2 \\ \hat{v}_1 \\ \hat{v}_0 \end{bmatrix} = \underbrace{\begin{bmatrix} 0 & 0 & -1/L_1 & 0 \\ 0 & 0 & 0 & -1/L_2 \\ 1/C_1 & 0 & 0 & 0 \\ 0 & 1/C_0 & 0 & -1/RC_0 \end{bmatrix}}_{A_2} \begin{bmatrix} i_1 \\ i_2 \\ V_1 \\ V_0 \end{bmatrix} + \underbrace{\begin{bmatrix} 1/L_1 \\ 0 \\ 0 \\ 0 \end{bmatrix}}_{B_2} [V_g] \text{ and}$$

$$\hat{x} = [A_2]x + [B_2]u$$

and for a full interval: circuit averaging concept is used as under

$$[A] = [A_1]d + [A_2](1-d) \text{ and } [B] = [B_1]d + [B_2](1-d)$$

$$\begin{bmatrix} \hat{i}_1 \\ \hat{i}_2 \\ \hat{v}_1 \\ \hat{v}_0 \end{bmatrix} = \begin{bmatrix} 0 & 0 & -(1-d)/L_1 & 0 \\ 0 & 0 & d/L_1 & -1/L_2 \\ (1-d)/C_1 & -d/C_1 & 0 & 0 \\ 0 & 1/C_0 & 0 & -1/RC_0 \end{bmatrix} \begin{bmatrix} i_1 \\ i_2 \\ V_1 \\ V_0 \end{bmatrix} + \begin{bmatrix} 1/L_1 \\ 0 \\ 0 \\ 0 \end{bmatrix} [V_g]$$

$$\dot{x} = [A]x + [B]u \text{ and } y = [C]x + [D]u$$

Small Signal analysis has been done with adding small perturbation in all state(s) as under:

$$i_1 = I_1 + \hat{i}_1, \quad i_2 = I_2 + \hat{i}_2, \quad v_1 = V_1 + \hat{v}_1, \quad v_0 = V_0 + \hat{v}_0 \text{ and } d = D + \hat{d}$$

The state space equations would transformed as shown below:

$$\frac{d}{dt} \begin{bmatrix} I_1 + \hat{i}_1 \\ I_2 + \hat{i}_2 \\ V_1 + \hat{v}_1 \\ V_0 + \hat{v}_0 \end{bmatrix} = \begin{bmatrix} 0 & 0 & -1/L_1 & 0 \\ 0 & 0 & 0 & -1/L_2 \\ 1/C_1 & 0 & 0 & 0 \\ 0 & 1/C_2 & 0 & -1/RC_2 \end{bmatrix} \begin{bmatrix} I_1 \\ I_2 \\ V_1 \\ V_0 \end{bmatrix} + \begin{bmatrix} 0 & 0 & -1/L_1 & 0 \\ 0 & 0 & 0 & -1/L_2 \\ 1/C_1 & 0 & 0 & 0 \\ 0 & 1/C_2 & 0 & -1/RC_2 \end{bmatrix} \begin{bmatrix} \hat{i}_1 \\ \hat{i}_2 \\ \hat{v}_1 \\ \hat{v}_0 \end{bmatrix} + \begin{bmatrix} 1/L_1 \\ 0 \\ 0 \\ 0 \end{bmatrix} [V_g] + \begin{bmatrix} 1/L_1 \\ 0 \\ 0 \\ 0 \end{bmatrix} [\hat{v}_g]$$

$$\begin{bmatrix} \{(D + \hat{d}) + L_2(V_1 + \hat{v}_1)/L_1L_2 \\ \{(D + \hat{d}) - L_2(V_1 + \hat{v}_1)/L_1L_2 \\ \{(D + \hat{d}) - (I_1 + i_1) + (I_2 + i_2)/C_1 \\ 0 \end{bmatrix} + \begin{bmatrix} 1/L_1 \\ 0 \\ 0 \\ 0 \end{bmatrix} [V_g] + \begin{bmatrix} 1/L_1 \\ 0 \\ 0 \\ 0 \end{bmatrix} [\hat{v}_g]$$

and

$$\frac{d}{dt} \begin{bmatrix} \hat{i}_1 \\ \hat{i}_2 \\ \hat{v}_1 \\ \hat{v}_0 \end{bmatrix} = \begin{bmatrix} 0 & 0 & -(1-D)/L_1 & 0 \\ 0 & 0 & -d/L_2 & -1/L_2 \\ 1-d/C_1 & d/C_1 & 0 & 0 \\ 0 & 1/C_2 & 0 & -1/RC_2 \end{bmatrix} \begin{bmatrix} \hat{i}_1 \\ \hat{i}_2 \\ \hat{v}_1 \\ \hat{v}_0 \end{bmatrix} + \begin{bmatrix} 1/L_1 \\ 0 \\ 0 \\ 0 \end{bmatrix} [V_g] + \begin{bmatrix} 1/L_1 \\ 0 \\ 0 \\ 0 \end{bmatrix} [\hat{v}_g]$$

$$\begin{bmatrix} V_1/L_1 \\ -V_1/L_1 \\ (I_2 - I_1)/C_1 \\ 0 \end{bmatrix} + \begin{bmatrix} 1/L_1 \\ 0 \\ 0 \\ 0 \end{bmatrix} [\widehat{v}_g] + \text{Steady state}$$

The small signal equations are further be translated into transfer function and from above equations Open loop transfer functions are derived and Transfer functions are derived for its stability and audio susceptibility.

Transfer function = $[C] [sI - A]^{-1}[B]$, where

$$[A] = \begin{bmatrix} 0 & 0 & -(1-d)/L_1 & 0 \\ 0 & 0 & -d/L_2 & -1/L_2 \\ (1-d)/C_1 & d/C_1 & 0 & 0 \\ 0 & 1/C_2 & 0 & -1/RC_2 \end{bmatrix} \quad [B] = \begin{bmatrix} V_1/L_1 \\ V_1/L_1 \\ (I_2 - I_1)/C_1 \\ 0 \end{bmatrix}$$

$$[X] = \begin{bmatrix} 1/L_1 \\ 0 \\ 0 \\ 0 \end{bmatrix}$$

(a) Control to output transfer function : ($\widehat{V}_g = 0$)

$$\frac{\widehat{i}_1}{d} = [1 \ 0 \ 0 \ 0][sI - A]^{-1}[B], \quad \frac{\widehat{i}_2}{d} = [0 \ 1 \ 0 \ 0][sI - A]^{-1}[B] \text{ and}$$

$$\frac{\widehat{v}_0}{d} = [0 \ 0 \ 0 \ 1][sI - A]^{-1}[B]$$

(b) Line to output transfer function (Audio Susceptibility): $\widehat{d} = 0$

$$\frac{\widehat{v}_0}{vg} = [0 \ 0 \ 0 \ 1][sI - A]^{-1}[B]$$

Since Solar PV array has variable power production based on irradiance and temperature of solar cell. To control the output, the Cuk converter has been analyzed using state space equations and tested for its stability analysis [51]. The simulation has compared the system with a compensation scheme to minimize output voltage deviation in response to change in the input voltage of the system. The state space modeling and its analysis supports in the design of controller needs the detailed stability and feasibility analysis.

Cuk converter has been chosen to provide better output voltage with reduced ripples and increased efficiency. MPPT methods are used in solar PV systems to extract the maximum power from the PV array under dynamic atmospheric conditions.

The performance of Cuk converter which is connected with the MPPT controller and a solar panel with standard value of irradiance and temperature, has been included in the simulation circuit. From the results obtained from simulation, incremental conductance method is found to be the optimum MPPT for extracting the maximum power. From the comparison, Cuk converter topology with incremental conductance controller offers better output voltage along with high voltage gain and efficiency. Hence usage of efficient power Cuk converter in solar PV system has been used and provides better solution to meet the energy demand.

2.2.2. MATLAB Simulation of PV Module

For any grid-connected PV system, two stage conversions has been reported first, a DC converter to extract maximum power from panel and convert the voltage from the array to close to the grid voltage. Second stage is an inverter is used to convert from DC to AC and sync it up with the grid, as schematic shown in Figure 2.14. A detailed SIMULINK Model has been created for a real industrial site location 1 and simulation study has been conducted. The Jindal make modules with specification mentioned in Table 2.2 has been used for two modules connected to form an array of 500 W of nominal maximum power.

Table 2.2. Electrical specifications of Jindal Solar one module

Electrical Characteristics	Values
Maximum Power (P_{max})	250 W
Voltage at P_{max} (V_{mp})	36.0 V
Current at P_{max} (I_{mp})	6.94 A
Short-circuit Current (I_{sc})	8.2 A
Open-Circuit Voltage (V_{oc})	43.0 V
Temperature coefficient of I_{sc}	$0.065 \pm 0.015\%/^{\circ}\text{C}$
Temperature coefficient of Power	$-0.5 \pm 0.05\%/^{\circ}\text{C}$
Nominal operating cell temperature (NOCT)	$40 \pm 2^{\circ}\text{C}$
Max. System Voltage	400 V

The simulation of model as in Figure 2.14 have been given in Chapter 5 [41].

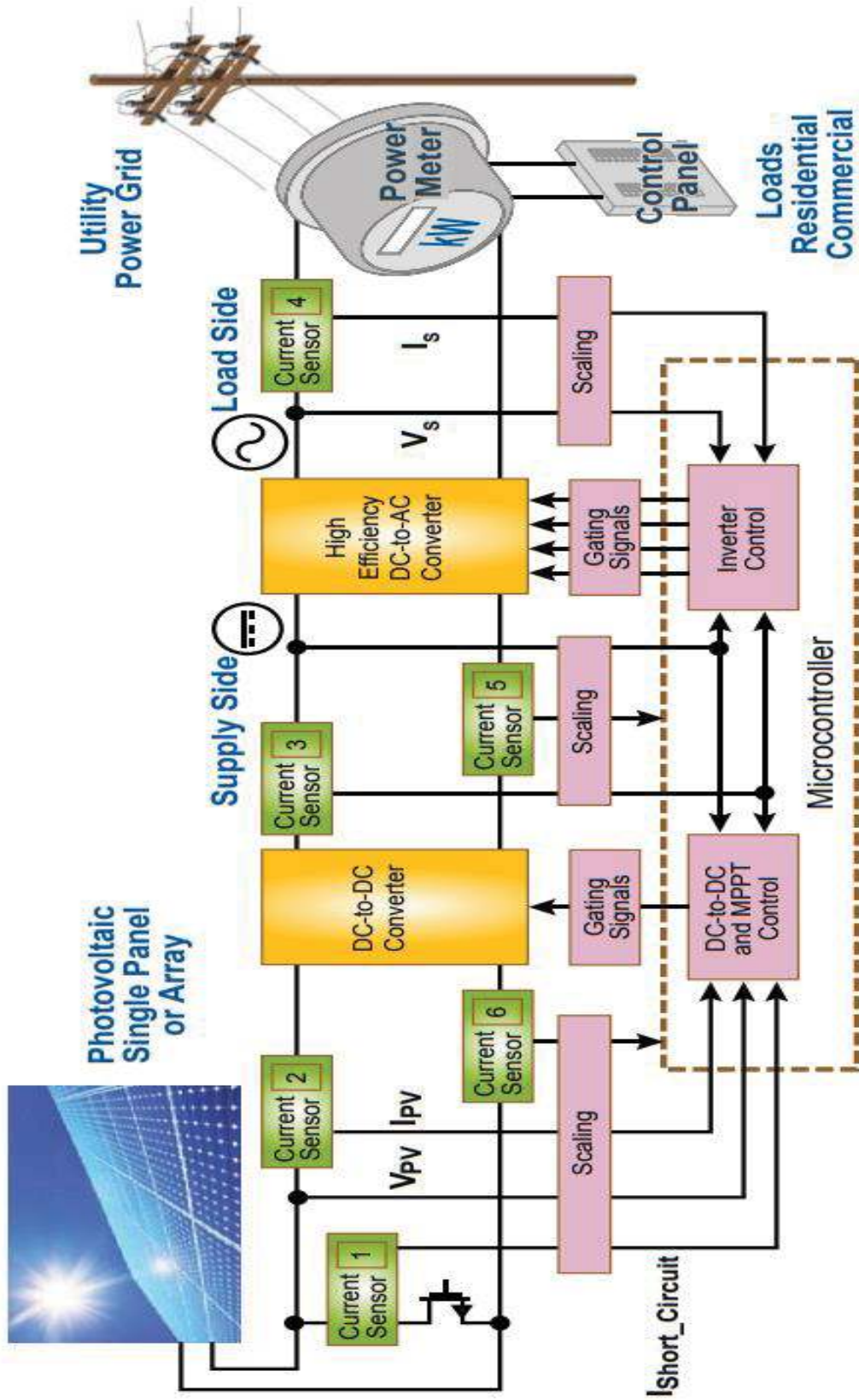


Figure. 2.14. Schematic single line diagram-PV array to grid [41]

India has been facing major challenges in substantial emission reduction and slow growth of RE sources. It has been reported that an energy mix is necessary by the year 2050 as summarized in Table 2.3 [52].

Table 2.3. Global Energy Mix by 2050 to achieve 450 ppm CO₂e

Exajoules (in a Year)	Current Energy Mix	Energy Mix in 2050				
	Global	Global	USA	EU	China	India
Energy Type	% of the total					
Coal without CCS ¹	26	2	1	1	4	3
Coal with CCS	0	9	9	7	20	20
Oil	34	18	20	25	15	14
Gas without CCS	21	19	20	20	10	7
Nuclear	6	8	8	9	9	8
Biomass without CCS	10	12	12	9	10	15
Non Biomass	3	10	8	9	9	12
Total	493	700	98	60	120	65

Due to volatile nature of solar insolation, the generation of solar electricity becomes very difficult to control. In this work the concept, design and methodology of 'Dispatcher control system' has been discussed, which optimizes the energy balance between solar electricity and grid electricity. Another impact of volatility of solar power is that during some periods of time, solar electricity goes unused and for other time periods not able to fulfill the requirements. This unique thought of a control system emerges, by which user controls its consumption with respect to the grid power and solar electricity.

A MATLAB™ based dispatcher module system has been designed which balances solar generation and grid power consumption. The control system predicts the PV generation based on the geographical location and weather forecast. The specific study at location1, generated PV power be optimized and keep grid power available for sale. The START and STOP of the equipment would be on the availability of free energy (Solar Energy). This phenomenon often called, 'Solar Power Generation Prognosis' has been used to control energy consumption, it refers that non-essential devices will start their work when the

¹ CCS: Carbon Capture and Storage

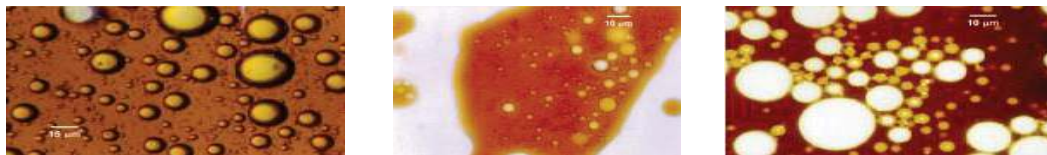
generation covers their needs and essential devices would continuously work on grid power and PV power. As referred in the section 2.1, aggressive energy efficiency solution, CSP has been targeted another focused research.

2.3. Commercial application of Concentrated Solar Power (CSP)

In today's era when RE sources are being explored exhaustibility and used for energy security, Oil and Gas industry is a major producer as well as consumer of energy. This sector has been projected to have dominance to support the world energy demand for minimum next two decades [53].

The extracted crude oil from earth crust commonly termed as 'Emulsion' is processed to separate from various mixture and contamination. The Emulsion is mainly classified as first oil-in-water emulsion, and second, water-in-oil emulsion [54]. Emulsions classifications as shown in Figure 2.15, need heating at the first stage of crude oil processing using designed Heater Treater chambers and thick-oil loses their bonding. Another solution like Gravity settling methods also gives better results however heating solutions increases crude droplet size and finally toward coalescence.

This research work has attempted the methods of crude oil heating like, traditional NG based, grid supply, Solar PV system and finally biomass-Solar based hybrid system. The research study concludes that the application of solar energy for the 'Crude Oil Heating' in the oil and gas industry has revealed an excellent opportunity for future business of the renewable energy industry and these opportunities include the use of photovoltaic and solar thermal technologies.



(a) Water-in-oil emulsion. (b) Presence of solids (c) Water-in-oil-water

Figure. 2.15. Emulsion classifications and its Photomicrographs [55]

The conceptualized 'State of Art' research studies have been explained in the Chapters 4 and 5 respectively. The study primarily focused on the use of Solar Energy for the crude oil heating purpose besides lower carbon footprint. The heating process of emulsion requires the pre-heat temperature in the desired range utilizing solar energy technology which has capability of

developing high-grade temperature exchange system. Further, to cater the sustainable energy, bioenergy has been emerged as dual role of producing high yield biomass and effective for carbon capture simultaneously.

2.4. Microalgae application for Carbon Sequestration

Microalgae based bioenergy resources have been emerged as a promising solution for energy security challenges worldwide and are advantageous due to their high photosynthetic response.

The microalgae have also been reported as potential bio-source to capture the carbon emissions and its conversion to value added co-products like biofuels, biogas, nutrients, etc. The present work has been focused on microalgae based Carbon capture from an industrial location 3 and utilizing the bio gas for creating a hybrid system with the existing crude oil heating process. ‘State Of Art’ research Bio-fixation of GreenHouseGases (GHG)-CO₂ with microalgae has been utilized at ONGC’s gas processing complex at location 3.

Pilot scale algae sequestration using culture column and raceway pond were analyzed for ‘Chlorella’ species with industrial vent gas [56]. The vent gas contributes towards supply of CO₂ for the culture and the produced biogas is utilized in hybrid system for oil heating. The associated PV system has been utilized for electrical power needs.

The hybrid system of Biomass-Solar-Natural Gas module has been analyzed for techno-economic aspects. The energy-mass balance confirms the productivity of algal biomass matches with heat requirement of crude oil heating system and the hybrid solutions are an effective method for sustainable future of Oil and Gas industry.

2.5. Conclusions

This chapter has been focused on RE resources for reducing carbon emissions and energy security in associated industrial applications in ONGC India. Solar PV power optimization has been targeted for a location 1. Aspect of utilizing CSP technology for crude oil heating has been briefed for location 2. Microalgae have been also targeted with close connection for environmental sustainability and CO₂ sequestration process has been firmed for location 3.

In the next chapter the specific utilization of Solar Energy and Bio-Energy Resources in Oil and Natural Gas industries has been deliberated in detail.